Excitational energy transfer enhancing ionization and spatial-temporal evolution of air breakdown with UV laser radiation

Jason S. Hummelt[a] and John E. Scharer
Department of Electrical and Computer Engineering, University of Wisconsin, Madison, Wisconsin 53706, USA

(Received 12 August 2010; accepted 18 September 2010; published online 5 November 2010)

This paper examines the role multiphoton excitation of oxygen has on the ionization of nitrogen in laser air breakdown. Plasma is created by focusing a 193 nm ArF excimer laser using an 18 cm focal length lens, producing a cylindrical 540 μm wide spot of intensity 6.5 GW/cm^2, well below the classical limit for collisional cascade (CC) breakdown. By spectroscopically monitoring the B $^2\Sigma_u^+$ to X $^2\Sigma_g^+$ transition at 391.4 nm of N_2^+ in N_2 and O_2 mixes, collisions between N_2 and metastable O_2 states that have undergone 1+1 absorption processes are shown to lower the degree of nonlinearity (i.e., the number of photons involved in the rate limiting multiphoton absorption process) in the ionization of N_2. This process is also found to dominate the 2+1 resonant enhanced multiphoton ionization of N_2 in air and be the primary source for ionization of N_2 to the B $^2\Sigma_u^+$ state. Plasma formation and evolution is also examined using a 1.3 cm focal length objective lens creating a 40 μm wide spot of intensity 1.25 TW/cm^2, above the classical limit for breakdown. This plasma is imaged with a fast (1.2 ns) gating intensified charge coupled device camera. Early plasma formation is seen to be inhomogeneous in nature, and significant ion density is found to exist up to 20 μs after the laser pulse. © *2010 American Institute of Physics*. [doi:10.1063/1.3504243]

I. INTRODUCTION

Air breakdown at high frequencies (microwave and above) is an important process in many industrial, military, and medical applications.[1,2] Breakdown at 193 nm is particularly important because of the widely used ArF transition in many excimer lasers used in the semiconductor manufacturing industry, and there is an increasing demand to move to shorter wavelengths for industrial applications such as photolithography.[3] In CC breakdown ionization occurs via the production of secondary electrons from the collisions of neutrals with high energy electrons that have been accelerated by electromagnetic fields present. Accelerated electrons will produce secondary electrons after undergoing a collision with a neutral atom that has an ionization energy lower than the energy of the electron. In this process, initial electrons are necessary to seed the breakdown process. In optical and shorter wavelength lasers, breakdown via the classical avalanche process is seeded and enhanced by multiphoton processes, whereas in microwave or IR lasers (such as CO_2 lasers $\lambda = 10.6$ μm) classical breakdown must be seeded by random causes such as cosmic rays, and at atmospheric pressure and sea level background electron production has an ionization rate of 10 cm^{-3}/s.[4] Quantum seeding can have ionization rates many orders of magnitude greater than this,[5] and thus short wavelength lasers prove to be promising for seeding ionization via other conventional breakdown mechanisms (i.e., microwaves), as well as providing a seed for their own fields as well. Our previous work has shown that multiphoton ionization (MPI) and resonance enhanced MPI (REMPI) quantum ionization processes act as a seed for classical CC breakdown in nitrogen. Density, temperature, and shock wave velocity measurements have been made on plasmas created with the 193 nm excimer laser and 1.3, 2, and 18 cm focal length lenses in both air and nitrogen.[5–7] In this paper air breakdown is further analyzed by investigating the role oxygen has on the ionization of N_2 in an air discharge utilizing an 18 cm focal length lens to achieve breakdown. It was hypothesized that while REMPI processes are responsible for some of the ionization and CC seeding of N_2 in air and all of it in pure N_2, REMPI of nitrogen is not the most important process involved in the ionization and seeding of CC of N_2 in air. This was initially evidenced by the observation that the emission of the N_2^+ first negative band head intensity at 391.4 nm was easily detectable in air but nearly disappeared in a pure N_2 environment.

This paper also presents images of breakdown with a 1.3 cm focal length objective lens that was imaged with a fast gating (1.2 ns) intensified charge coupled device (ICCD) camera. The 1.3 cm focal length objective lens produces a much denser (10^{18} cm^{-3} compared to 10^{16} cm^{-3} as measured by two color laser interferometry) and hotter (nearly all N_2 converted to atomic N) plasma than the 18 cm focal length lens.[5]

Gas dynamics have a major impact on plasma evolution in plasmas created via moderate (GW/cm^2 range) intensity lasers, and the plasma parameters are highly transient in nature and very dependent on laser intensity, photon energy, background gas, and pressure.[8] Despite its fundamental nature, much remains to be discovered about plasma evolution in air and other gases due to the complex nature of the topic which causes a difficult analytic and computational analysis of the processes involved. Thus we have utilized plasma im-

[a]Electronic mail: hummelt@mit.edu.

aging on fast timescales (1.2 ns) to serve as a useful diagnostic to aid in the understanding of plasma evolution and formation.

II. BACKGROUND

A. Collisional cascade breakdown

In the microwave range, quantum effects can be ignored and electrons absorb energy from an electromagnetic field classically via inverse bremsstrahlung. Although ionization at optical and even UV laser wavelengths includes other ionization processes, cascade ionization still plays a large role in the total ionization process and it is necessary to incorporate it into the overall breakdown picture.[6,7] In cascade ionization, electrons gain energy by absorbing photons while in the presence of a third body. The creation of secondary electrons through collisions with atoms or molecules is then governed by the equation[9]

$$\nu_i = n_0 \langle \sigma_i \cdot \omega_e \rangle, \tag{1}$$

where ν_i is the ionization frequency, n_0 is the neutral density, σ_i is the electron neutral collision cross section, and ω_e is the electron drift velocity. Visible breakdown occurs at an electron density n_e significantly higher than the background electron density of air. If the initial electron density is taken to be 10^5 cm^{-3} in atmospheric air (as is assumed by Smith and Meyerand[10]) and breakdown is taken to mean a final density of 10^{15} cm^{-3}, one can arrive at a formula for the threshold intensity required for breakdown via CC processes by combining the integrated form of the continuity equation and the electron absorption equation, and assuming an energy loss frequency to excitation of nitrogen[2] of 10^9 s^{-1} to obtain

$$I_{Bd\ CC} = \left(\frac{8 \times 10^2}{P t_p \lambda^2}\right)(1 + 4.5 \times 10^{-6} P^2 \lambda^2) \times (1 + 2 \times 10^7 t_p P), \tag{2}$$

where the laser intensity is in watt per square centimeter, t_p is the laser pulse duration in seconds, λ is the radiation wavelength in microns, and p is the pressure in atmospheres. Although this gives a good qualitative picture for the breakdown mechanism, the actual process is more complicated, especially in the case of a high intensity laser. The electron energy distribution, which is in general not Maxwellian, determines the ionization rate and electron losses. However, net growth of electron density is not controlled by the average energy electrons as has been assumed in the previous analysis, but by electrons occupying the tail of the distribution function with enough energy to remove subsequent electrons.[10] Because in general shorter wavelength lasers produce many more "hot" electrons at the end of the electron distribution tail than microwaves,[9] one anticipates a lowering of the intensity required for breakdown in the case of a laser.

B. MPI and REMPI

As already stated, quantum ionization processes introduced by high energy photons need to be accounted for in the total picture of ionization using a short wavelength laser. In general, the ionization energy of most diatomic molecules is greater than even the energy produced by UV lasers. Thus UV lasers fall short of direct photoionization. However, at these higher energies MPI becomes increasingly possible, and in cases where there is a high photon flux (as in the case of a laser) there can be a high probability for an MPI event to occur. When an atom or molecule absorbs enough photons such that the sum of their energies is greater than the ionization potential of the atom or molecule in a small enough amount of time, called the excitation lifetime, ionization will occur. The excitation lifetime $\tau = h/\varepsilon_i$ is determined from Heisenberg's uncertainty principle, where h is Planck's Constant and ε_i is the photon energy. Based on the theory laid out by Tozer,[11] if a region is irradiated by a laser beam containing n_0 atoms/cm^3 in a laser pulse duration T, then n_e electrons/cm^3 will be produced such that

$$n_e = \frac{n_0 T}{\tau} \frac{(n_v \cdot \tau \cdot \sigma)^m}{m} \exp[-n_v \cdot \tau \cdot \sigma], \tag{3}$$

where n_v is the photon flux, τ is the excitation lifetime, σ is the one neutral photoabsorption cross section, and m is the degree of nonlinearity. The degree of nonlinearity can be found from the relation[12]

$$m = \frac{d\ \log[A^+]}{d \log I}, \tag{4}$$

where $[A^+]$ is the total number of ions created and I is the laser intensity.

If a molecule in a laser field has a resonant state near an integer multiple of the laser photon energy, it is then possible for the atom to absorb enough photons to get to the resonant state and subsequently absorb enough photons to ionize it. This process is known as REMPI.[13] This process is very important for any MPI event involving three or more photons as in general the decay constant of the resonant state is much longer than the excitation lifetime within which the atom must absorb photons (femtoseconds as compared with nanoseconds or longer), and the greater number of photons needed to get above the ionization threshold the smaller the probability for ionization. For an m+k REMPI process the degree of nonlinearity will be the rate limiting process, or for m > k the degree of nonlinearity will be m. Shown in Fig. 1 is an energy level diagram of a molecule depicting a 2+1 REMPI process.

1. Effective cross sections

For an m photon MPI event, the ionization rate W scales like[10]

$$W = \sigma_m I^m, \tag{5}$$

where I is the intensity of the laser pulse, W is the ionization rate, σ_m is the total photoabsorption cross section, and m is once again the degree of nonlinearity. Thus it is possible to deduce a photoabsorption cross section if the intensity of the laser pulse and density of the plasma are known. It will also be useful to develop an "effective cross section" for a given gas species as the introduction of an additional gas species will change the chemistry involved in ionization.

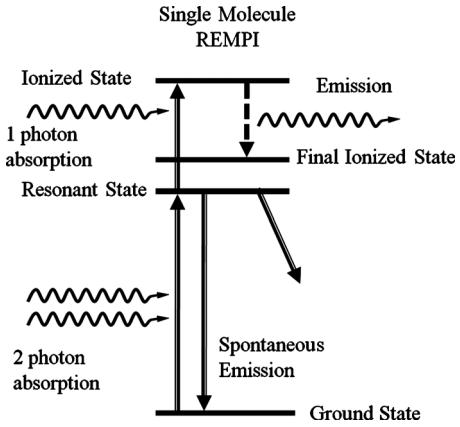

FIG. 1. 2+1 REMPI process shown in an energy level diagram. The molecule absorbs two photons to reach a resonant state, from which it absorbs one more to ionize. From the ionized state the molecule then emits a photon to reach a final ionized state, before it will decay back down to the ground state. This 2+1 REMPI process is seen in N_2 with 193 nm laser radiation, where the ionized N_2^+ emits at 391 nm to decay from the ionized $^2\Sigma_u^+$ state (Ref. 5).

C. Collisional enhancement in air breakdown

The dynamics of air breakdown with a 193 nm laser are further complicated by the complex chemistry involved. Although the many trace molecular and atomic species found in air all contribute to the breakdown process, the role of nitrogen and oxygen in air breakdown is of prime importance due to the large concentrations of both diatomic molecules. Thus it is crucial to understand the interactions between the two molecules that influence the ionization process.

In a molecular collision energy exchange is more complex than in atomic collisions due to the fact that the translational energy of one species can be transferred to one of the internal motion energies of the other (i.e., vibrational and rotational energy states). In the gas temperature range of 100 to 5000 °K, vibrational and/or rotational state excitation from the translational motion of other molecules is a characteristic process, and electronic transitions from collisions will only occur to a significant degree at higher temperatures.[14]

Thus most of the energy exchanged between O_2 and N_2 in an air plasma from the translational motion of the two molecules will be given to raise the rotational and vibrational temperatures of various states, and vibrational to translational energy exchange will keep the plasma in thermal equilibrium over longer time scales.[15,16] Even though normally not important in breakdown not utilizing beams or lasers, collisions inducing electronic transitions can occur if a metastable state transfers its electronic energy to another molecule via a collision.[17]

In the case of a laser plasma, specific metastable states of molecules can be excited, and they may become heavily populated in the plasma created. Moreover, where quantum absorption processes occur, very few states may be involved and this can result in a few nearly filled metastable states. These metastables act as excellent energy reservoirs from which energy can be released at a later time. Metastables may be able to transfer their energy to other species in the discharge via collisions, work to heat the background gas, or

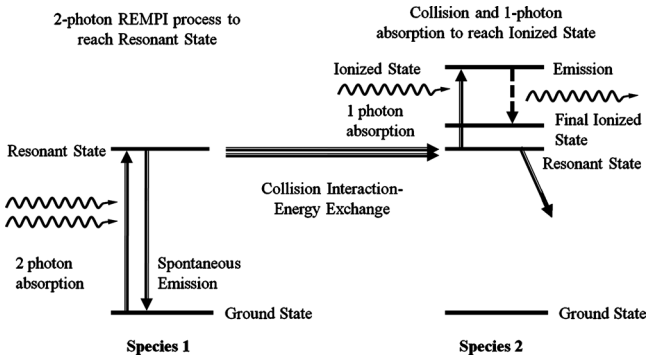

FIG. 2. Energy level diagram of two molecules where species one absorbs 2 photons and transfers that energy to species two via collisional excitation energy transfer. The second molecule then subsequently absorbs an additional photon to become ionized and decays down to a final ionized state as seen in the 2+1 REMPI process discussed earlier.

be ionized at a later time via electron impact ionization.[18] Of interest to those studying discharges involving quantum ionization in the presence of multiple species is electronic energy transfer to other molecules via collisions. This can be described by the equation

$$M^* + A + mh\nu \rightarrow M^* + A \xrightarrow{\text{Collision}} M + A^*, \tag{6}$$

where m is the degree of nonlinearity in the multiphoton event.

Energy transfer from a metastable state in water with metastables in nitrogen have been documented by Laufer *et al.*[17] Utilizing a 248 nm KrF laser they discovered that after absorbing 2 photons, H_2O in the $\tilde{C}^1B_1[OH(B\ ^2\Sigma_u^+)+H(^2S)]$ state was exciting the 2 photon resonant states involved in the REMPI of N_2 (including the a $^1\Pi_g$, a′ $^1\Sigma_u^-$, and w $^1\Delta_u$ states near 10 eV). If a molecule has a higher cross section for absorption of radiation, it can assist in ionizing molecules with lower cross sections through collisions. In gas mixtures where this occurs a complex REMPI process involving more than one species of gas and collisional energy transfer can arise. Shown in Fig. 2 is an energy diagram depicting such a process.

III. EXPERIMENTAL SETUP

A. 193 nm excimer laser

The experimental setup has been described in earlier work,[5–7] but a brief description is given here for clarity. 193 nm laser radiation is created by a Lumonics Pulsemaster PM-842 ArF excimer laser. The laser pulse is 20 ns in duration and has an energy of 310 mJ per pulse with a fresh gas fill. The output beam is rectangular, 2.5×1 cm^2, which is then shaped by two fused silica lenses to a square 1×1 cm^2 beam for focusing. One of two focusing lenses (f=18 cm or f=1.3 cm) is then used to focus the beam in a pressurized laser chamber. The chamber has four window ports, with a CaF_2 glass window for optimal transmission of the 193 nm laser. The attenuation through the window was measured to be 7%, and the attenuation constant of the 193 nm laser radiation through air was measured to be 2.6 m. Gas flow into the chamber is controlled by an MKS PR4000B, which

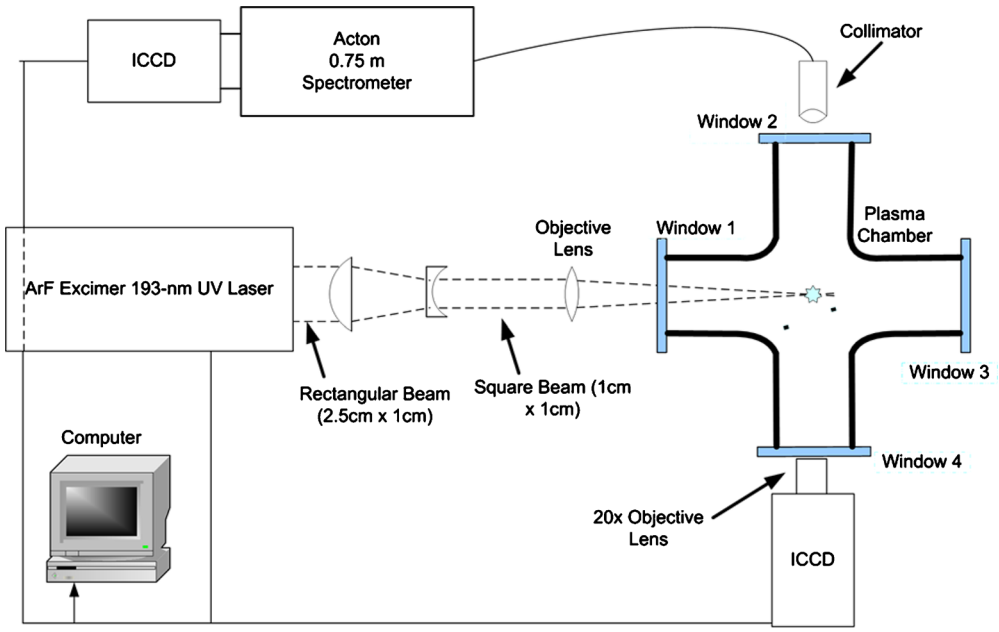

FIG. 3. (Color online) Experimental setup of 193 nm ArF laser experiment focused in a pressure and gas species controlled chamber. Experimental diagnostics include a fast ICCD camera as well as a spectrometer for optical spectroscopy measurements. Timing and triggering of all devices is controlled by a remote computer utilizing LABVIEW software.

subsequently sets and monitors the flow rate on two MKS M100B Mass-Flo Controllers. Each of these controllers has a range of up to 200 SCCM (SCCM denotes cubic centimeter per minute at STP) and were used to control the flow of N_2, O_2, and air into the chamber while a MKS PDR900–1 monitored the pressure. A mechanical scroll pump with the ability to produce a base pressure of 20 mTorr was used to pump on the chamber and the pump rate could be set to match the flow rate into the chamber to keep it at a constant pressure. A diagram of the experimental setup is shown in Fig. 3.

One of the lenses used for breakdown is a fused silica lens with a focal length of 18 cm. This lens has an antireflection coating that transmits 97.7% of 193 nm laser radiation. Using the equation for the focal spot size of an ideal lens $r=\Theta^{*}f/2$ where r is the spot size radius, Θ is the laser beam divergence (3 mrad for our laser), and f is the focal length, one arrives at a spot size of 540 μm in diameter. This lens thus produces an intensity of 6.5 GW/cm^2 in the 20 ns laser pulse. The lens itself has a diameter of 3.8 cm and so is able to focus all incident light from the 1×1 cm^2 laser beam. The second lens is an OFR LMU-15×-193 objective lens with a focal length of 1.3 cm. The spot size is determined to be 40 μm in diameter as this is what is experimentally observed from the early ICCD images of the plasma formation where the focused laser beam waist is still visible. This lens thus produces an intensity of 1.25 TW/cm^2 in the 20 ns laser pulse. Shown in Fig. 4 is the intensity required for CC breakdown compared to the intensity of both the 18 and 1.3 cm focal length lenses, illustrating the fact that the 18 cm focal length lens produces fluxes well below the CC breakdown threshold whereas the 1.3 cm lens produces fluxes above it.

B. Plasma imaging

Fast camera images were taken of the plasma using an Andor I-Star DH-734 ICCD camera. The camera is able to gate down to 1.2 ns, which is very useful for capturing plasma dynamics. In order to check this value, the gain of the camera was adjusted until the point where the image would "bleed out" (saturate with too much light from the plasma) with a gate of 1.2 ns. Then the gate was increased by 0.1 ns increments until significant bleeding occurred at 1.5 ns. This method proved that the camera does indeed gate with times less than 1.5 ns, and so the quoted value of 1.2 ns is reasonable [Fig. 5].

A 20× objective microscope lens was attached to the ICCD camera to magnify the image of the plasma. The camera has a physical pixel size of 26 μm per pixel and a resolution of 1024 pixels×1024 pixels Therefore the 20× lens produced images with 1300 nm per pixel and a total image area of 1.3×1.3 mm^2.

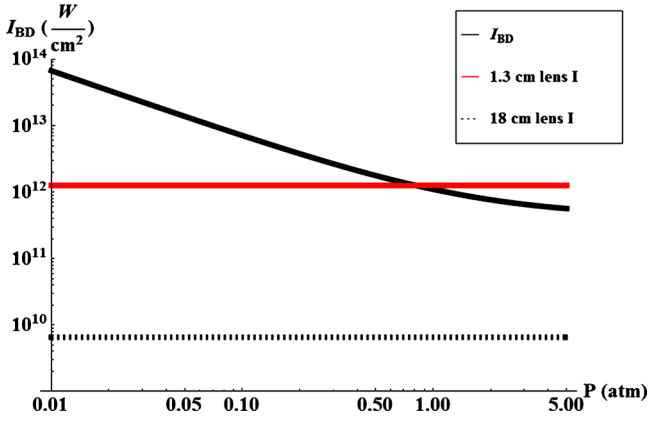

FIG. 4. (Color online) Intensity required for CC breakdown in air compared with the intensity of both an 18 and 1.3 cm focal length lens. Note that at 1 atm the 1.3 cm lens is above the threshold required for breakdown and the 18 cm is more than two orders of magnitude below.

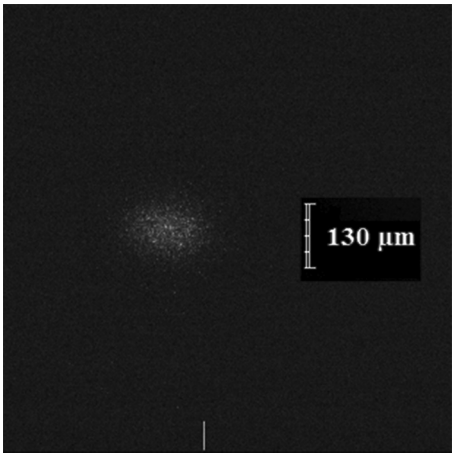

FIG. 5. Plasma formation at t=−10 ns. A gate time of 1.2 ns is used. It is interesting to note the inhomogeneous nature of the plasma at very early times.

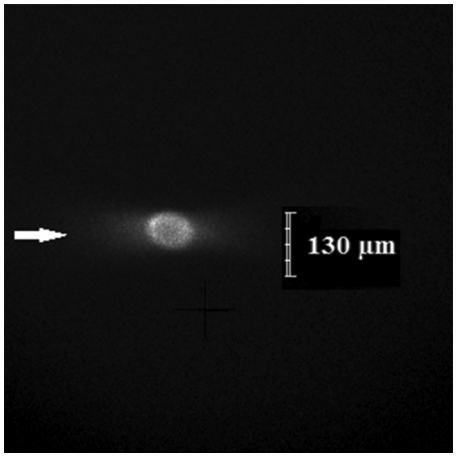

FIG. 6. Plasma formation at t=0 ns right before the laser pulse has ended. A gate time of 1.2 ns is used. The waist of the beam is 40 μm in diameter.

C. Optical spectroscopy

A collimator consisting of two different lenses was built to capture light from the plasma. The lenses were chosen and spaced to have a focal length of 30 cm, enough distance to put the collimator outside the pressurized chamber, but close enough to still provide a large enough solid angle to capture as much of the light emitted as possible. The physical diameter of the collimator is 2.5 cm, so that the collimator covers roughly 0.044% of the solid angle surrounding the plasma emission. The light is focused onto a broadband optical fiber that transmits light from 200–800 nm with <1% loss. The light was then subsequently split by an Acton SpectraPro spectrometer with a 75 cm focal length. This was then focused onto the ICCD to measure the output intensity. The ICCD has a quoted spectral range of 360–1080 nm

The spectrometer system was used to measure breakdown intensity of nitrogen by monitoring the N_2^+ first negative band head at 391.4 nm. This is the strongest emission line found in aurorae and is caused by nitrogen in the upper atmosphere interacting with electromagnetic radiation.[19,20]

IV. RESULTS

A. Plasma imaging

Plasma formation with a 1.3 cm focusing lens was documented using a 20× microscope focusing objective mounted to an ICCD camera in Figs. 5–9. Uncertainty in the timing of the laser and ICCD system caused a ±1 ns timing uncertainty in the images taken relative to the laser fire. Time 0 is defined as starting at the end of the 20 ns laser pulse, i.e., a time of −5 ns is 5±1 ns before the end of the laser pulse and a time of 5 ns is 5±1 ns after the end of the pulse. The laser is incident from the left hand side, as indicated by the white arrow in Fig. 6. All images are scaled equally in size with the same gain.

At early times the plasma is very inhomogeneous and many "microdischarges" are formed around the focal spot of the lens. It is interesting to note that the initial plasma density does not all start in center of the focal spot of the lens but only becomes concentrated here as additional ionization occurs. This could be attributable to a soft self-focusing effect that the plasma density has on the laser light. Self-focusing has been shown to refocus laser light providing an enhancement of light intensity in air plasmas for high intensity lasers.[18] As the plasma becomes more dense toward the end of the laser pulse and the ion density toward the center of the focal spot of the lens grows, the plasma expands from here until hundreds of nanoseconds after the laser pulse. The plasma then becomes very diffuse with visible ion density radiating out until t=20 μs. At the low light intensities encountered this far into the plasmas life, the spatial characteristics of the plasma become harder to determine as noise in the ICCD itself will start to have an effect on the observed image [Figs. 7].

B. Concentration of N_2/O_2 scaling

As the N_2-O_2 collision frequency changes, the ionization of N_2 will change as well. Air breakdown is complex due to both the chemistry and physics involved, and much can be learned about breakdown phenomena simply by studying the attributes of breakdown as a function of gas properties-such as pressure and specie concentration. As has been shown, MPI processes can act as a seed for CC processes at UV and shorter wavelengths.[5,21] Here we discuss

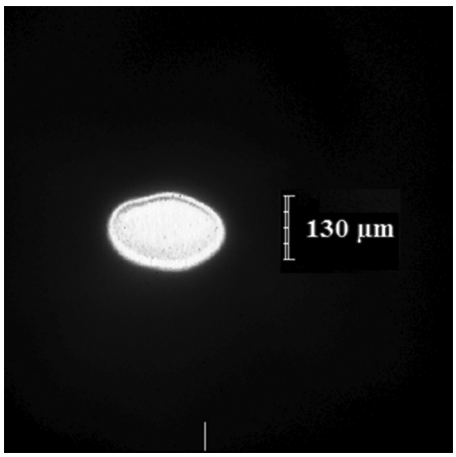

FIG. 7. Plasma formation at t=20 ns. A gate time of 1.2 ns is used.

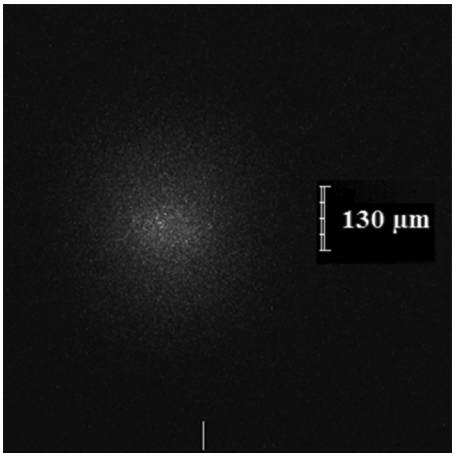

FIG. 8. Plasma formation at t=5 μs. A gate time of 100 ns is used as the plasma is emitting less light.

the effect a foreign species experiencing MPI or REMPI has on the MPI or REMPI of another species. Collisional effects between O_2 and N_2 enhancing the REMPI signal of the N_2^+ first negative system at 391.4 nm in a plasma created with 193 nm laser radiation are examined. First the concentration of O_2 in pure N_2 was varied and the spectroscopic signal from N_2^+ at 391.4 nm was monitored as the laser energy was varied. As was shown before, the degree of nonlinearity can be obtained from Eq. (4) by taking the slope of the log-log plot of the N_2^+ first negative signal versus laser energy. Plotted in Fig. 10 are the results of this measurement taken in a mix of 90% N_2 and 10% O_2.

Measurements were also taken in mixes of 50% N_2 and 50% O_2, 70% N_2, and 30% O_2, and dry air which has a mixture of 78.4% N_2, 20.9% O_2, 0.9% Ar, and a few other trace gases. In the 50% N_2 mix a degree of nonlinearity of 1.77 with a correlation coefficient of 97% was found, the 70% N_2 mix produced a degree of nonlinearity of 1.93 with a correlation coefficient of 97%, and air yielded a degree of nonlinearity of 2.00 with correlation coefficient of 96%. All measurements were taken at 50 Torr where quantum ionization processes dominate collisional cascade ionization processes.[22]

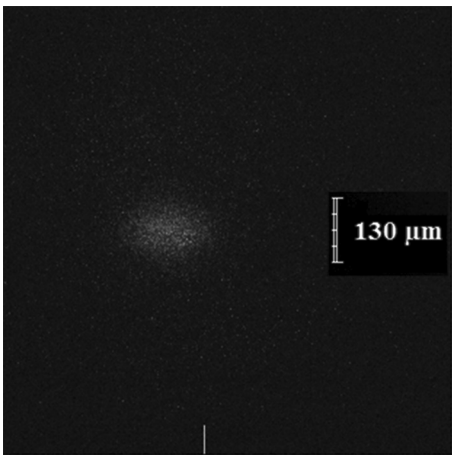

FIG. 9. Plasma formation at t=20 μs. A gate time of 100 ns is used.

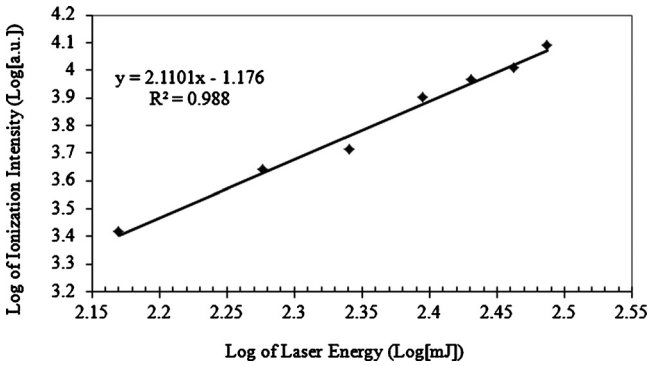

FIG. 10. Log-log plot of breakdown intensity vs varying laser intensity in a mix of 90% N_2 and 10% O_2 at 50 Torr. The plot yields a degree of nonlinearity of 2.11 with a correlation coefficient of 99%.

The reason the degree of nonlinearity shrinks by adding oxygen in a nitrogen discharge is threefold. First, collisional quenching between states works to bring down the degree of nonlinearity as it competes with the processes filling the B $^2\Sigma_u^+$ state in nitrogen.[23] Second, intense radiation can cause the upper levels of atoms or molecules to shift and broaden to overlap the continuous spectrum, effectively lowering the ionization potential of the atom.[10] Third, and most importantly, because oxygen can undergo a 1+1 photon absorption to a metastable state[24] and transfer this energy to nitrogen via collisions, this will decrease the degree of nonlinearity in the ionization of N_2. The latter of these three processes is most important for our experiments because all measurements are taken at 50 Torr so that the N_2 quenching rate will be the same in all three experiments,[22] and the effect of the laser radiation in shifting the upper energy levels of the N_2 molecule will be the same regardless of the presence of O_2.

The collisional effects between N_2 and O_2 in air were further examined by monitoring the N_2^+ first negative system band head intensity as a function of N_2 concentration for 50, 100, and 200 Torr where multiphoton processes become decreasingly important in direct ionization, but are still important in providing seeding for CC processes. The results are shown in Fig. 11.

All the breakdown curves peak for a given concentration of N_2 and then slowly taper off as the N_2 concentration is

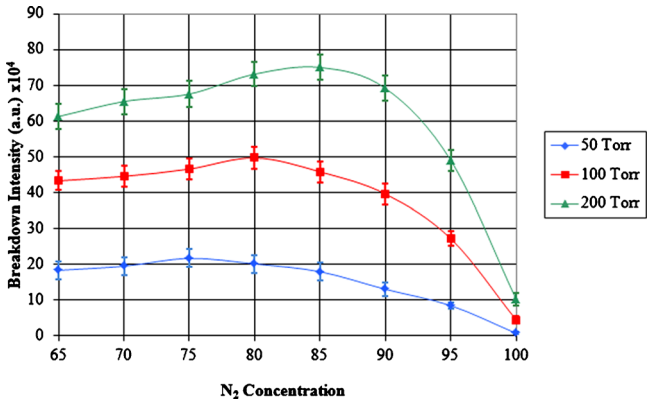

FIG. 11. (Color online) Optical breakdown intensity of the N_2^+ first negative band head at 391.4 nm as a function of N_2 concentration in a N_2/O_2 mix for three different pressures: 50, 100, and 200 Torr.

reduced. It is clear that a simple 2+1 REMPI process involving just nitrogen is not the main driver behind B $^2\Sigma_u^+$ nitrogen ion formation in air plasmas created with 193 nm laser radiation, as the effect of adding just 5% of molecular oxygen has a significant impact on molecular nitrogen ion formation.

One possibility for the mechanism of energy transfer between oxygen and nitrogen is the transfer of electronic energy from the metastable states involved in the REMPI of O_2. At 193 nm O_2 reaches the $O_2^+X\ ^2\Pi_g$ ground electronic state via a 1+1 REMPI process after autoionization from the metastable $ns\sigma_g(n-1)d\pi\ ^1_g\Sigma_g^+$ Rydberg series. The molecule's resonant state in the 1+1 process occurs at the B $^3\Sigma_u^-$ state.[24] The two photon resonant state in N_2 has been observed at the a $^1\Pi_g$ state for 193 nm laser radiation in N_2.[5,13] As the $ns\sigma_g(n-1)d\pi\ ^1_g\Sigma_g^+$ Rydberg series in O_2 and the a $^1\Pi_g$ state in N_2 lie at the same energy level, the resonant O_2 molecules occupying the Rydberg series have the ability to transfer energy to N_2 molecules during collisions to raise them to the a $^1\Pi_g$ state. From here an N_2 molecule can subsequently absorb a photon to reach the ionized B $^2\Sigma_u^+$ state. The 1+1 REMPI process in oxygen will dominate the 2 photon absorption because of the longer lived B $^3\Sigma_u^-$ state in O_2.

Another possibility for energy exchange is direct charge transfer from O_2^+ molecules that have absorbed 3 photons. Resonant oxygen states that have absorbed 1+1+1 photons will autoionize to the A $^2\Pi_u$ and a $^4\Pi$ states, both of which are a few electron volts lower than the energy of three 6.42 eV photons (19.26 eV) and the B $^2\Sigma_u^+$ state. Since the charge transfer reaction between O_2^+ and N_2 is nonresonant (the energy to ionize N_2 to the B $^2\Sigma_u^+$ state is more than the energy of the two O_2^+ A $^2\Pi_u$ and a $^4\Pi$ states), this reaction has a small probability of occurring in our low temperature plasma.[25] Therefore, the most probable of the two energy transfer mechanism to N_2 is electronic excitation from collisions with O_2^+ in the $ns\sigma_g(n-1)d\pi\ ^1_g\Sigma_g^+$ Rydberg series.

It is difficult to distinguish between the relative strengths of the electronic excitation from O_2 versus the direct REMPI of N_2 in the overall REMPI signal of the 391.4 nm band head. Although the quenching rate should be small as the pressure is low, it has been observed that the a $^1\Pi_g$ state in nitrogen is linked to the a′ $^1\Sigma_u^-$ state in nitrogen via collisional quenching, and will have a small effect on the experimentally measured degree of nonlinearity for all mixtures of nitrogen and oxygen.[26] This nonlinear process is difficult to separate out from the direct REMPI of nitrogen and the excitational energy exchange between oxygen and nitrogen. It will need to be corrected for before any quantitative statements can be made about the relative strengths of the other two multiphoton effects. Therefore, at this time we can only qualitatively conclude that collisional energy exchange from oxygen metastables is dominant in the ionization of nitrogen in laser air breakdown at 193 nm.

C. Pressure scaling

The collisional effects between N_2 and O_2 in air were further examined by monitoring the N_2^+ first negative system band head intensity as function of pressure for various mixtures of N_2 and O_2, as well as air. These experiments explore the ionization of N_2 up to higher pressures where quantum processes become less important for direct ionization of N_2 but are still important for seeding. The results are shown in Fig. 12.

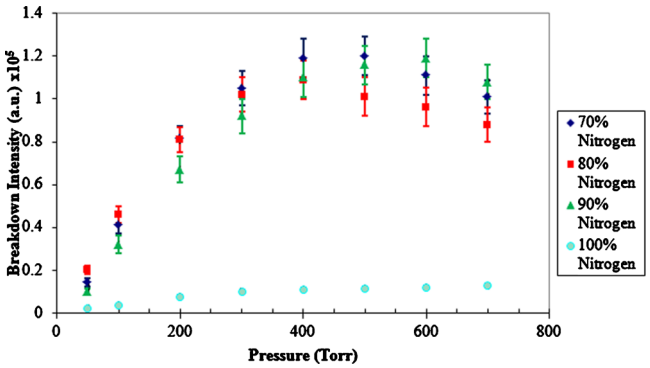

FIG. 12. (Color online) Breakdown intensity of the 391.4 nm emission from the N_2^+ first negative system as a function of pressure for different concentrations of O_2 in N_2.

V. CONCLUSIONS

The dynamics of air breakdown at 193 nm with a sub-CC breakdown threshold laser of focused intensity 6.5 GW/cm^2 have been examined. It has been shown that with the addition of oxygen in N_2, 2+1 REMPI of N_2 is not the main ionization process for N_2 and is also not the main ionization process acting on N_2 in air. Collisional excitational energy transfer via collisions from oxygen metastables are shown to enhance quantum ionization processes in air breakdown at wavelengths where these quantum processes are the primary means for molecular absorption of laser energy. While 2+1 REMPI of nitrogen is still existent in air breakdown at 50 Torr, 1+1 REMPI of oxygen is found to lower the degree of nonlinearity for ionization of N_2. Excitational energy transfer to N_2 through collisions of the $ns\sigma_g(n-1)d\pi\ ^1_g\Sigma_g^+$ resonant Rydberg series in O_2^+ are found to aid in the ionization of N_2 to produce N_2^+ ions.

In addition, plasma temporal and spatial evolution in air with an above CC breakdown threshold laser of focused intensity 1.25 TW/cm^2 were imaged with a fast gating ICCD camera using gate widths down to 1.2 ns. The plasma is seen to evolve inhomogeneously from localized microspots forming during the laser pulse which merge together near the end of the laser pulse. Ion density is seen to exist past 20 μs.

ACKNOWLEDGMENTS

Research supported by AFOSR Grant No. FA9550-09-1-0357.

[1] A. D. MacDonald, *Microwave Breakdown in Gases* (Wiley, New York, 1966), pp. 1–5, Vol. 111–120.
[2] N. Kroll and K. Watson, Phys. Rev. A **5**, 1883 (1972).
[3] V. Liberman, M. Rothschild, J. H. C. Sedlacek, R. S. Uttaro, A. Grenville, A. K. Bates, and C. Van Peski, Opt. Lett. **24**, 58 (1999).
[4] Y. P. Raizer, *Laser-Induced Discharge Phenomena* (Consultants Bureau, New York, 1997), pp. 53–57.
[5] J. Way, J. Hummelt, and J. Scharer, J. Appl. Phys. **106**, 083303 (2009).

[6]M. Thiyagarajan and J. Scharer, J. Appl. Phys. **104**, 013303 (2008).
[7]M. Thiyagarajan and J. E. Scharer, IEEE Trans. Plasma Sci. **36**, 2512 (2008).
[8]S. S. Harilal, C. V. Bindhu, M. S. Tillack, F. Najmabadi, and A. C. Gaeris, J. Phys. D: Appl. Phys. **35**, 2935 (2002).
[9]S. Soubacq, P. Pignolet, E. Schall, and J. Batina, J. Phys. D: Appl. Phys. **37**, 2686 (2004).
[10]G. Bekefi, *Principles of Laser Plasmas* (Wiley, New York, 1976), pp. 457–467.
[11]B. A. Tozer, Phys. Rev. **137**, A1665 (1965).
[12]G. Baravian, J. Godart, and G. Sultan, Appl. Phys. Lett. **36**, 415 (1980).
[13]J. Bominaar, C. Schoemaecker, N. Dam, J. J. Ter Meulen, and G. C. Groenenboom, Chem. Phys. Lett. **435**, 242 (2007).
[14]W. H. Miller, *Modern Theoretical Chemistry* (Plenum, New York, 1976), pp. 131–206.
[15]M. I. Boulos, P. Fauchais, and E. Pfender, *Thermal Plasmas: Fundamentals and Applications* (Plenum, New York, 1994), pp. 164–170.
[16]H. K. Shin, J. Chem. Phys. **55**, 5233 (1971).
[17]G. Laufer, A. S. Lee, and H. K. Chelliah, Appl. Opt. **36**, 3278 (1997).
[18]V. Guerra, P. A. Sa, and J. Loureiro, J. Phys. D: Appl. Phys. **34**, 1745 (2001).
[19]P. Swings, Publ. Astron. Soc. Pac. **60**, 18 (1948).
[20]G. Sun, E. Ott, Y. C. Lee, and P. Guzdar, Phys. Fluids **30**, 526 (1987).
[21]L. J. Radziemski and D. A. Cremers, *Laser-Induced Plasmas and Applications* (Marcel Dekker, New York, 1989), pp. 1–5.
[22]Y. P. Raizer, *Gas Discharge Physics* (Springer-Verlag, Berlin, 1991), pp. 144–159.
[23]G. Laufer, R. H. Krauss, and J. H. Grinstead, Opt. Lett. **16**, 1037 (1991).
[24]B. L. G. Bakker and D. H. Parker, J. Chem. Phys. **112**, 4037 (2000).
[25]M. Lieberman and A. Lichtenberg, *Principles of Plasma Discharges and Materials Processing* (Wiley, New York, 2005), pp. 240–262.
[26]P. J. Dagdigian, Annu. Rev. Phys. Chem. **48**, 95 (1997).